Multistep Nature of Microvascular Recruitment of Ex Vivo–expanded Embryonic Endothelial Progenitor Cells during Tumor Angiogenesis

Peter Vajkoczy,[2] Sabine Blum,[1] Mathias Lamparter,[1] Reinhard Mailhammer,[1] Ralph Erber,[2] Britta Engelhardt,[3] Dietmar Vestweber,[3,4] and Antonis K. Hatzopoulos[1]

[1]*GSF-Research Center for Environment and Health, Institute for Clinical Molecular Biology and Tumor Genetics, 81377 Munich, Germany*
[2]*Department of Neurosurgery, Klinikum Mannheim, University of Heidelberg, 68167 Mannheim, Germany*
[3]*Max-Planck Institute for Vascular Biology, 48149 Münster, Germany*
[4]*Institute of Cell Biology, ZMBE, University of Münster, 48149 Münster, Germany*

Abstract

Tissue neovascularization involves recruitment of circulating endothelial progenitor cells that originate in the bone marrow. Here, we show that a class of embryonic endothelial progenitor cells (Tie-2$^+$, c-Kit$^+$, Sca-1$^+$, and Flk-1$^-$/low), which were isolated at E7.5 of mouse development at the onset of vasculogenesis, retain their ability to contribute to tumor angiogenesis in the adult. Using intravital fluorescence videomicroscopy, we further defined the multistep process of embryonic endothelial progenitor cell (eEPC) homing and incorporation. Circulating eEPCs are specifically arrested in "hot spots" within the tumor microvasculature, extravasate into the interstitium, form multicellular clusters, and incorporate into functional vascular networks. Expression analysis and in vivo blocking experiments provide evidence that the initial cell arrest of eEPC homing is mediated by E- and P-selectin and P-selectin glycoprotein ligand 1. This paper provides the first in vivo insights into the mechanisms of endothelial progenitor cell recruitment and, thus, indicates novel ways to interfere with pathological neovascularization.

Key words: intravital fluorescence videomicroscopy • neovascularization • cell trafficking • PSGL-1 • selectins

Introduction

Circulating endothelial progenitor cells (EPCs),* mobilized from the bone marrow into the blood stream, contribute to new blood vessel formation and, thus, promote neovascularization during tissue ischemia, vascular trauma, and tumor growth (1–10). However, the molecular and cellular mechanisms underlying EPC recruitment and differentiation are not yet understood, and remain as one of the central issues in stem cell biology (11). For instance, it is unclear how circulating EPCs specifically home to angiogenic sites, which critical steps underlie their incorporation into new blood vessels, and how effectively these processes compare with the activation of local, preexisting endothelial cells (12).

A hindering factor for a systematic analysis of EPC homing mechanisms is the fact that adult EPCs are difficult to isolate, maintain, and genetically manipulate in vitro. Therefore, in this paper, we investigated the mechanisms of homing and incorporation of EPCs during new blood vessel formation in a tumor model using mouse embryonic EPCs (eEPCs) as a model system (13). The major advantages of eEPCs are their robust growth properties in culture and practical genetic manipulation. The eEPCs express early endothelial markers, differentiate to mature endothelial cells, form vascular tubes in vitro, and build blood vessels after transplantation during embryogenesis (13). Their gene expression profile (*tie-2*, *thrombomodulin*, *GATA-4*, *GATA-6*, etc.) matches the pattern observed in

Address correspondence to Antonis K. Hatzopoulos, GSF-Research Center for Environment and Health, Institute for Clinical Molecular Biology and Tumor Genetics, Marchioninistrasse 25, 81377 Munich, Germany. Phone: 49-89-7099-214; Fax: 49-89-7099-225; E-mail: hatzopoulos@gsf.de

**Abbreviations used in this paper:* DiI, 1,1′-dioctadecyl-3,3,3′,3′-tetramethylindocarbocyanine perchlorate; EGFP, enhanced green fluorescent protein; EPC, endothelial progenitor cell; eEPC, embryonic EPC; PECAM-1, platelet–endothelial cell adhesion molecule-1; PSGL-1, P-selectin glycoprotein ligand 1; RT, reverse transcriptase; VEGF, vascular endothelial growth factor.

 J. Exp. Med. © The Rockefeller University Press • 0022-1007/2003/06/1755/11 $8.00
Volume 197, Number 12, June 16, 2003 1755–1765
http://www.jem.org/cgi/doi/10.1084/jem.20021659

the proximal lateral mesoderm that will give rise to the embryonic endocardium and myocardium. However, the isolated cells do not express, or are not induced to express under a variety of conditions, early myocardial-specific genes (*Nkx2.5* or *MLC2a*) and, thus, appear committed to the endothelial lineage. This notion is further supported by transplantation studies in embryos that showed differentiation of these cells only toward the endothelial lineage and no other emerging cell types were observed (13). Extensive flow cytometry analysis with a large number of antibodies (e.g., against tie-2, c-kit, VE-cadherin, CD44, etc.), showed that the in vitro–expanded embryonic cells constitute a homogeneous population (unpublished data).

Based on these properties, we were able to use eEPCs in the powerful intravital fluorescence videomicroscopy technique to visualize the fate of circulating enhanced green fluorescent protein (EGFP)– or DiI-labeled eEPCs during tumor angiogenesis. This experimental approach allowed us first to demonstrate that ex vivo–expanded eEPCs can contribute to tumor-induced blood vessel growth in the adult, and, second, to define the multistep interaction of eEPCs with angiogenic tumor blood vessels. The results provide a first insight into the mechanisms underlying recruitment, homing, and vascular incorporation of EPCs as a basis for the design of novel means to therapeutically manage angiogenic processes.

Materials and Methods

Isolation and Labeling of eEPCs. The procedures for the isolation and ex vivo expansion of the eEPCs from E7.5 mouse embryos, as well as their differentiation with cAMP and retinoic acid, have been described previously in detail (13). We fluorescently labeled the isolated eEPCs either by the lipid soluble dye DiI (1,1′-dioctadecyl-3,3,3′,3′-tetramethylindocarbocyanine perchlorate; Molecular Probes; references 14, 15) or by genetic labeling using an EGFP (CLONTECH Laboratories, Inc.) construct under the phosphoglycerate kinase promoter. To this end, 1.5–2.0 $\times$ 10^7 eEPCs were suspended in 20 ml HSB (25 mM Hepes, pH 7.1, 134 mM NaCl, 5 mM KCl, and 0.7 mM Na_2HP0_4), washed once with 10 ml HSB, centrifuged, resuspended in 0.8 ml HSB buffer, and transferred to a 0.8-ml electroporation cuvette. We added 30 μg of plasmid DNA and placed the cells on ice for 10 min. eEPCs were electroporated at 350 V, 500 μF using a Gene Pulser II (Bio-Rad Laboratories) and were placed on ice for 10 min. The electroporated cells were transferred to 24 ml of culture medium and plated. The next day, we started selection with 200–400 μg/ml G418 (Invitrogen) and proceeded for 10–14 d, exchanging medium daily. Colonies were picked and expanded for further analysis.

RNA Analysis. We prepared RNA using the isolation kit from QIAGEN and reverse-transcribed total RNA into cDNA as follows: 1 μg RNA was mixed with 100 ng oligo$(dT)_{15}$ and incubated for 5 min at 65°C. 1 mM dNTPs, 60 mM KCl, 15 mM Tris-Cl, pH 8.4, 3 mM $MgCl_2$, 0.3% Tween 20, 10 mM β-mercaptoethanol, 10 U RNasin (Promega), and 100 U Mo-MLV RT (Invitrogen) were added, and the mix was incubated for 55 min at 37°C followed by a second incubation period of 5 min at 95°C. Reverse transcriptase (RT)–PCR was performed with 20 ng cDNA using Taq DNA polymerase (Promega) for 30–35 cycles (1 min at 95°C, 1 min at 60–65°C, and 1 min at 72°C). The primer sequences were as follows: flk-1, 5′-ggaATTCAGGCATTGTACTGAGAG-3′, 5′-cggaTCCAAGTTGGTCTTTTCCTG-3′; tie-2, 5′-CAACAGCGTCTATCGGACTCC-3′, 5′-GAAAAGGCTGGGTTGCTTGATC-3′; von Willebrand Factor (vWF), 5′-ggaattcTGCTCAGTGGGGTGGATG-3′, 5′-cggatccGGGCTCACGTCCATGCGC-3′; c-Kit, 5′-GAGACGTGACTCCTGCCATCATG-3′, 5′-CATTTCGGCAGGCGCGTGCTC-3′; vascular endothelial growth factor (VEGF)-A, 5′-GGGTGCACTGGACCCTGGCT-3′, 5′-GAATTCACCGCCTCGGCTTGTC-3′; TGFβ, 5′-GAGACGGAATACAGGGCTTTCG-3′, 5′-CGGGTTGTGTTGGTTGTAGAGG-3′; GAPDH, 5′-CTCACTCAAGATTGTCAGCAATG-3′, 5′-GAGGGAGATGCTCAGTGTTGG-3′; aldolase, 5′-AGCTGTCTGACATCGCTCACCG-3′, 5′-CACATACTGGCAGCGCTTCAAG-3′; sca-1, 5′-GGTTGCAGCAGGCTATGCAAGCC-3′, 5′-CGGCTTCCTAGGTGCCAGGCC-3′ (16); E-selectin ligand, 5′-GCGGCTTCATGGATGACTGC-3′, 5′-ATGGTGTTCAATCTCCCCTCG-3′; P-selectin ligand, 5′-CCACCGTGGTCATGCTAGAG-3′, 5′-GACTTCGGTGGCTGCAGACG-3′; E-selectin, 5′-GCTGTCCAGTGTGAAGCCTTATC-3′, 5′-GCAATGAGGACGATGTCAGGA-3′; P-selectin, 5′-GCTTCAGGACAATGGACAGC-3′, 5′-CTTTCTTAGCAGAGCCAGGAGTG-3′; and ICAM-2, 5′-GGGTCTGGTGAGAAGGCCTTTGAGG-3′, 5′-GGGGACACCGTGCACTCAATGG-3′. Lowercase letters indicate nucleotides added for cloning purposes.

Tumor Model for Intravital Microscopy. We grew highly angiogenic rat C6 glioma tumor grafts within the skinfold chamber preparation of nude mice (NMRI nu/nu; $n = 10$), i.e., a transparent chamber model that allowed direct and noninvasive assessment of the tumor microcirculation using intravital microscopy (17, 18). Before tumor inoculation, the C6 cells were incubated with the fluorescent marker Fast Blue (Sigma-Aldrich) that allowed identification of the tumor mass by intravital microscopy at an excitation wavelength of 365 nm (19). After the tumors had established their microvascular system and initiated tumor growth (~50 mm^3) by day 10–14 after implantation, we inserted a polyethylene catheter (PE-10) into the right common carotid artery for systemic administration of fluorescent markers and injection of cells (19).

Intravital Fluorescence Videomicroscopy. We performed intravital multifluorescence videomicroscopy as described previously (14, 19, 20). Depending on the labeling technique for the eEPCs, we visualized individual microvessels by injection of either FITC- or rhodamine G–conjugated dextrans. This way, the distinct excitation wavelengths of the marker combinations allowed for localization of the eEPCs with respect to the blood vessel lumina. After visualization of the tumor microvasculature, 4 $\times$ 10^5 either DiI- or EGFP-labeled eEPCs suspended in 300 μl PBS, were infused in 100-μl aliquots. This protocol allowed us to assess the dynamic interaction between eEPCs and the tumor endothelium within three different microvascular regions (size $\approx$ 0.8 mm^2). To exclude recirculating cells from the analysis, we limited the observation period after cell injection to 20 s and waited for another 5 min to the next cell infusion. We repeatedly scanned the tumor microvasculature at 10 min, 1 h, 1 d, and 4 d after cell injection to assess permanent eEPC–endothelium interactions. At the end of these experiments, the heart, lung, liver, spleen, and pancreas were exposed in eight animals for intravital microscopic assessment of eEPC presence in these tissues. Chamber preparations without implanted tumors served as controls for the recruitment experiments ($n = 4$). Animals with tumors implanted into the skinfold chamber but injected with PBS instead of eEPCs

served as controls to address the consequences of eEPC injection on tumor vascularization and tumor growth ($n = 5$).

To study the role of P-selectin glycoprotein ligand 1 (PSGL-1) for eEPC recruitment to the tumor endothelium, we preincubated 4×10^5 DiI-labeled eEPCs with 215 μg 4RA10 (anti–mouse PSGL-1) in 500 μl PBS for 20 min ($n = 3$ animals). Subsequently, we centrifuged the eEPCs and washed them once with PBS before injection. To study the role of E-/P-selectin, we injected mice with 300 μg UZ4 (anti–mouse E-selectin) and 300 μg RB40.34 (anti–mouse P-selectin) in 200 μl PBS 20 min before the infusion of EPCs ($n = 3$). The monoclonal antibody MJ7/18 served as the control ($n = 3$) because it binds to the vascular wall without affecting endothelial cell adhesion and was successfully used as a control previously (20).

Intravital Microscopic Image Analysis. Quantitative analysis included the tumor area, total vessel density, diameter of individual blood vessels, mean blood flow velocity, shear rate, and shear stress (20, 21, 22). During cell injection, we determined the absolute number of eEPCs that passed through and were arrested within the microvascular region of interest. Furthermore, we separated cells that were permanently arrested within the microvasculature into adherent and plugging categories, depending on the mechanism of their arrest. We identified adherent eEPCs as cells that stuck to the vessel wall without moving or detaching from the endothelium, despite an unaltered microvascular blood flow. We defined plugging eEPCs as cells that were passively arrested either by blocking the lumen of small blood vessels or by being trapped within individual vascular sprouts. We quantified eEPC arrest as the number of adherent and plugging cells per area (mm^{-2}).

Hemodynamic parameters were quantitatively determined as described previously (22, 23). In brief, the quantitative analysis included the diameter of control postcapillary venules and tumor microvessels as well as the velocity of nonadherent EPCs. The highest cell velocity per venule, v_{max}, was used to calculate the mean blood flow velocity (μm/s): $v_{mean} = v_{max}/(2-\varepsilon^2)$, where ε is the ratio of the EPC diameter to vessel diameter (d). From v_{mean} and d, the wall shear rate ($\gamma[s^{-1}]$) was estimated as $\gamma = 8 \times v_{mean}$ /d and the shear stress (τ [dyne/cm^2]) was approximated by $\tau = \gamma \times 0.025$. Due to the high spatial resolution of the intravital microscopic technique, these analyses were performed not only for the individual tumor in general but also within different intratumoral areas (e.g., "hot spots" for eEPC adherence).

Subcutaneous Tumor Xenografts. To further study the influence of EPC injection on tumor growth, rat C6 glioma xenografts were grown subcutaneously after injection of 5×10^5 C6 cells into the left flank regions of nude mice (NMRI nu/nu). After the tumors had been established (by day 8 after implantation), 4×10^5 DiI-labeled eEPCs, suspended in 300 μl PBS, were infused into the animals ($n = 4$). Control animals were injected with PBS alone ($n = 4$). Tumor growth was assessed using vernier calipers until day 17 after implantation (i.e., as soon as weight loss started to exceed 20%). Tumor volume was calculated as (length × width × height)/2.

Detection of eEPCs by Immunofluorescence and Immunohistochemistry. We detected the eEPCs by immunofluorescence microscopy of serial frozen sections. Vessels containing eEPCs were counterstained with a monoclonal rat anti–mouse platelet–endothelial cell adhesion molecule-1 (PECAM-1) antibody (BD Biosciences), followed by staining with a goat anti–rat Cy3-conjugated IgG (Dianova). We performed immunohistochemistry on 6-μm frozen tumor sections as described previously (24).

Monoclonal Antibodies and Ig Chimeras. Mec13.3 (anti–mouse PECAM-1/CD31) was a gift from Dr. E. Dejana (Federazione Italiana per la Ricerca sul Cancro-Institute of Molecular Oncology, Milan, Italy; reference 25). The hybridomas Hermes-1 (= 9B5, anti–human CD44, used as an isotype-matched control), MECA-79 (anti–mouse PNAd), MECA-367 and MECA 89 (both anti–mouse MAdCAM-1), and MJ7/18 (anti–mouse endoglin) were obtained from American Type Culture Collection. RB40.34/4 (anti–mouse P-selectin), 4RA10 (anti–mouse PSGL-1), 10E9.6 (anti–mouse E-selectin), 25 ZC7 (anti–mouse ICAM-1), and 9DB3 (anti–mouse VCAM-1) were raised in D. Vestweber's laboratory; UZ4 (anti–mouse E-selectin; 26) provided by Dr. R. Hallmann (The Jubileum Institute, Lund, Sweden). 3C4 (anti–mouse ICAM-2) was purchased from BD Biosciences. E- and P-selectin IgG chimeras were raised in D. Vestweber's laboratory and described previously in detail (27, 28). The tie2 IgG chimera was a gift from Dr. U. Deutsch (Max-Planck Institute for Vascular Biology, Münster, Germany).

Flow Cytometry. Suspended eEPCs were incubated with 5 μg/ml anti–PSGL-1 mAb or purified rat IgG1 (BD Biosciences) in FACS® buffer (1% BSA and 0.1% NaN_3 in PBS) for 30 min on ice. Subsequently, eEPCs were washed twice and incubated with PE-conjugated anti–rat Ig in FACS® buffer and 5% mouse serum for 30 min. Analysis was performed on a Becton Dickinson FACSCalibur™. As a control, we used the mouse neutrophilic progenitor cell line 32DCl3 that stains positive for PSGL-1 with the same antibody (29). To test for the presence of E- and P-selectin ligands on the surface of eEPCs, we incubated 5×10^5–10^6 cells (eEPCs or peripheral blood cells as a positive control) with 80 μg/ml E- or P-selectin human IgG chimera in FACS® buffer supplemented with 2 mM Mg^{2+} and 2 mM Ca^{2+}. As a negative control for the chimeric molecules, we used a tie2-IgG chimera that does not bind to the cells. Specificity controls ensuring the lectin-mediated binding of the selectin-Ig constructs was tested in samples processed in parallel where Mg^{2+} and Ca^{2+} were replaced by 5 mM EDTA. Afterwards, we washed the cells twice with the corresponding buffers and incubated with 10 μg/ml PE-conjugated goat-anti–human IgG for 20 min at 4°C. We washed the cells twice, fixed them in 1% formaldehyde, and analyzed them on the FACSCalibur™.

Statistics. Quantitative data, except the size of the subcutaneous tumor xenografts, are given as mean values ± SD. Mean values were calculated from the average values in each animal. For analysis of differences between the groups, one-way analysis of variance followed by the appropriate post hoc test for individual comparisons between the groups was performed (ANOVA).

Results

eEPCs Retain Their Progenitor Properties after Ex Vivo Expansion. eEPCs were isolated, expanded in vitro, and fluorescently labeled in two different ways. In one approach, we electroporated the cells with an EGFP construct under the control of the phosphoglycerate kinase promoter, and stable transfected cell lines were established that produce EGFP (Fig. 1 A). In a second approach, we labeled cells with DiI (Fig. 1 B). Expression analysis of the ex vivo–expanded and –transfected cells revealed the typical expression pattern for endothelial markers as reported previously for freshly isolated eEPCs (Fig. 1 C; reference 13). Stimulation of transfected eEPCs with cAMP and retinoic acid confirmed their ability to differentiate to more mature en-

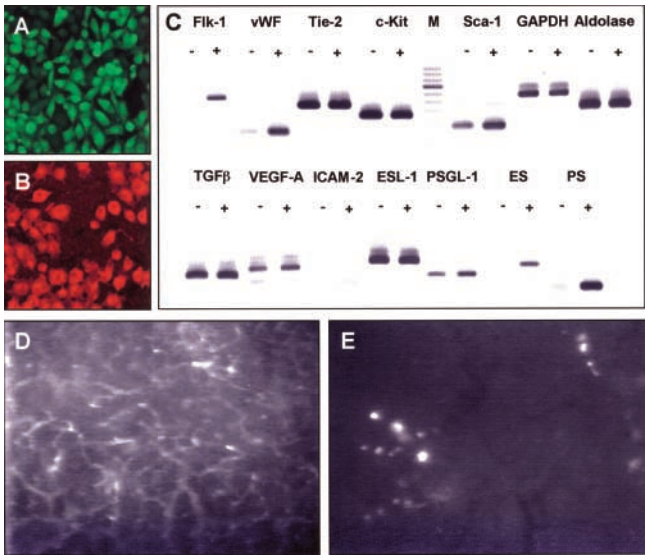

Figure 1. eEPCs home to tumor angiogenic sites. (A and B) Ex vivo–expanded eEPCs labeled with EGFP (A) or DiI (B). (C) RNA expression profiles by RT-PCR analysis in eEPCs before (−) and after activation (+) with cAMP and retinoic acid. M: 100 bp ladder molecular weight marker. The stronger band is 800 bp. (D) Tumor microvasculature on day 10 after implantation after contrast enhancement with rhodamine G–conjugated dextran. (E) EGFP-eEPCs are arrested heterogeneously within the tumor microvasculature after intraarterial injection. Same region of interest as in D.

dothelial cells (Fig. 1 C). This differentiation or activation of the eEPCs is accompanied by induction of flk-1, vWF, sca-1, and E- and P-selectin. Interestingly, unlike mature endothelial cells, eEPCs express angiogenic factors such as VEGF as well as the ligands for E- and P-selectin.

Ex Vivo–Expanded eEPCs Preferentially Home to Tumor Angiogenic Sites. Intravital microscopy of the tumor-free, nonangiogenic dorsal skinfold chamber tissue and of the highly angiogenic C6 glioma microvasculature demonstrated significant differences in the hemodynamic parameters (Table I). Although the control tissue was characterized by physiologic values, the tumor microvasculature displayed lower blood cell velocity, wall shear rate, and wall shear stress.

After infusion of ex vivo–expanded fluorescent eEPCs, we observed a comparable number of circulating cells (~100–200 per observation field) both within the tumor ($n = 10$ animals) and control microvasculature ($n = 4$ animals). Of those, 43 ± 18% and 7 ± 6% ($P < 0.05$) were permanently arrested within the lumen of tumor and control blood vessels. Moreover, eEPC arrest in tumors was remarkably heterogeneous in that the arrested cells preferentially homed to certain microvascular hot spots (Fig. 1, D and E). Importantly, all these regional differences in eEPC arrest were not attributable to regionally distinct hemodynamic conditions within the tumor microvasculature, indicating that this preferential arrest was not simply due to low blood flow in the hot spot areas (Table I).

Table I. *Microhemodynamic Parameters in Control Postcapillary Venules and Tumor Blood Vessels*

Blood vessel type	Diameter	Mean velocity	Wall shear rate	Wall shear stress
	μm	$\mu m/s$	s^{-1}	$dyne/cm^3$
Control	18.5 ± 3.5	705 ± 58	292 ± 28	7.3 ± 0.7
Tumor, in general	19.4 ± 3.8	348 ± 243[a]	159 ± 128[a]	4.0 ± 3.2[a]
Tumor, hot spots	18.0 ± 1.8	435 ± 338	193 ± 149	4.8 ± 3.7

Mean values ± SD are shown; microhemodynamic parameters were assessed in control blood vessels ($n = 4$ animals with tumor-free skinfold chambers), regular tumor blood vessels ($n = 6$ animals), and in tumor blood vessels representing hot spots of eEPC recruitment ($n = 5$ animals).
[a]*, $P < 0.05$ versus control.

eEPCs Actively Adhere to the Endothelium of Tumor Blood Vessels. Videomicroscopy revealed two mechanisms of permanent EPC arrest within tumor blood vessels. The majority of cells (87 ± 23%) actively adhered to the tumor endothelium without affecting blood flow in this vascular segment (Fig. 2, A–E). In contrast, the remaining cells (13 ± 23%) passively plugged tumor blood vessels by size restrictions or were trapped in dead-end vascular sprouts (Fig.

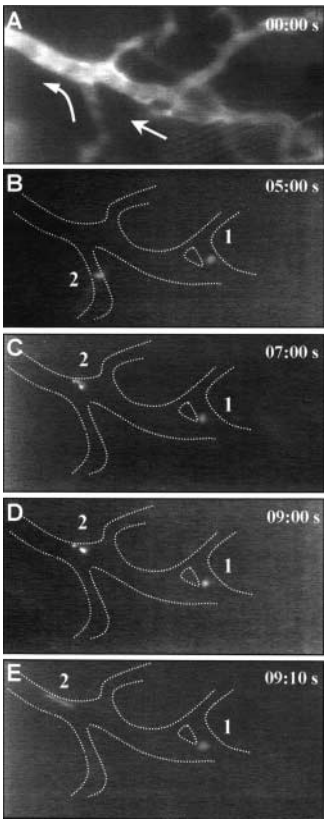

Figure 2. Circulating eEPCs interact with the tumor endothelium. (A) Tumor blood vessels before cell injection after contrast enhancement with FITC-conjugated dextran. Arrows indicate direction of microvascular blood flow. (B–E) Intravital microscopic sequence of two DiI-labeled eEPCs (1 and 2) interacting with the vessel wall of the identical vascular segment indicated in A. Cells adhere either permanently (1) or temporarily (2) to the endothelium. Numbers depict sequential time points in seconds (top right).

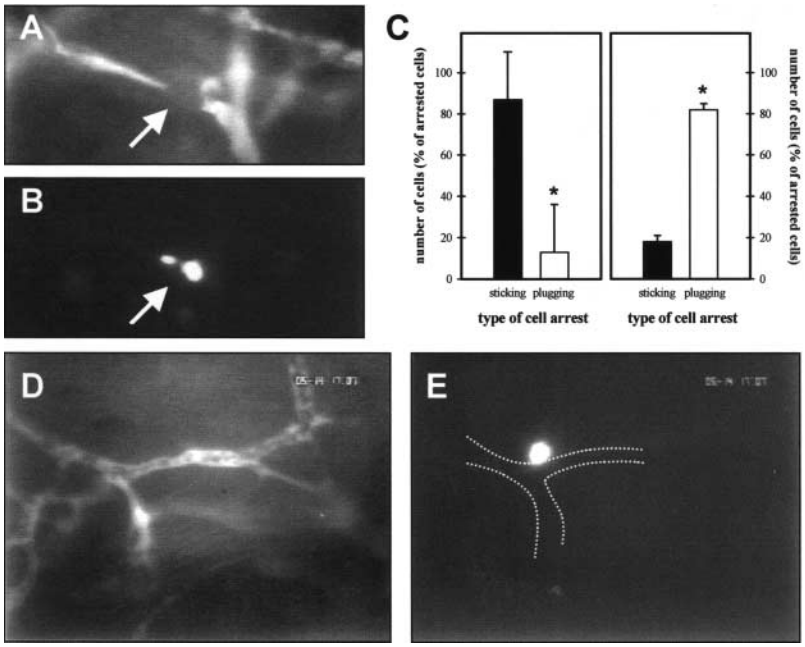

Figure 3. Mechanisms of eEPCs arrest in tumor and control tissue. (A and B) Narrow tumor blood vessel obliterated by plugging eEPC due to size restriction (arrows). Same region of interest in A and B. Tumor blood vessels and eEPCs are fluorescently marked as in Fig. 2. (C) Sticking versus plugging as mechanisms of eEPC arrest within tumor (left, $n = 10$ animals) and control (right, $n = 4$ animals) microvasculature. Control is chamber preparation without tumor implantation. Error bars show mean ± SD values. (D and E) Demonstration of eEPC migration through the endothelial lining within 1 h after intravascular arrest. Labeling of tumor blood vessels with rhodamine G–dextran (D) and of eEPCs with EGFP (E). Same region of interest in D and E. *, $P < 0.05$ versus control tissue.

3, A–C). In contrast, cells within control blood vessels were arrested predominantly by plugging the small caliber capillaries (3–5 μm; Fig. 3 C). This indicated clearly that active, permanent adhesion of eEPCs to blood vessel endothelium was a tumor-specific phenomenon.

Arrested eEPCs Extravasate and Form Multicellular Clusters within the Tumor Interstitium. Within 1 h, the arrested eEPCs started to extravasate from the tumor blood vessels (Fig. 3, D and E). After 1 d, all cells were localized in the extravascular space where they started to form multicellular clusters (Fig. 4, A and B). Higher magnifications revealed two types of cell morphology; 32% of the cells showed a round morphology (Fig. 4, C and D), whereas 68% became elongated and displayed a bipolar morphology (Fig. 4, E and F). Interestingly, the elongated cells were localized in the vicinity of active microvascular segments that displayed angiogenic sprouting. This was in contrast to the control tissue where only very few cells were localized extravascularly as single cells, and of those, only 29% displayed an elongated morphology.

eEPCs Contribute to Tumor Angiogenesis and Form Functional Blood Vessels. Within a few days, the extravasated and elongated eEPCs started to branch and form cellular networks. The double-labeling technique using fluorescent dextran to visualize functional (i.e., perfused) tumor blood vessels demonstrated clearly that these cells either formed microvascular sprouts (Fig. 5, A–C), or progressively spanned between individual vessels interconnecting distant microvascular segments (Fig. 5, D–F). Finally, multiple fluorescent cells lined perfused tumor blood vessels, indicating that recruited eEPCs had been successfully incorporated into the new tumor microvasculature (Fig. 6, A–D). Tumor cryosections stained with fluorescent antibodies against PECAM-1 confirmed the successful integration of injected eEPCs into the endothelial lining of the tumor microvasculature (Fig. 6 E).

eEPCs Preferentially Incorporate into Tumor Microvasculature. Quantitative analysis of eEPC homing demonstrated that circulating eEPCs preferentially homed to the tumor

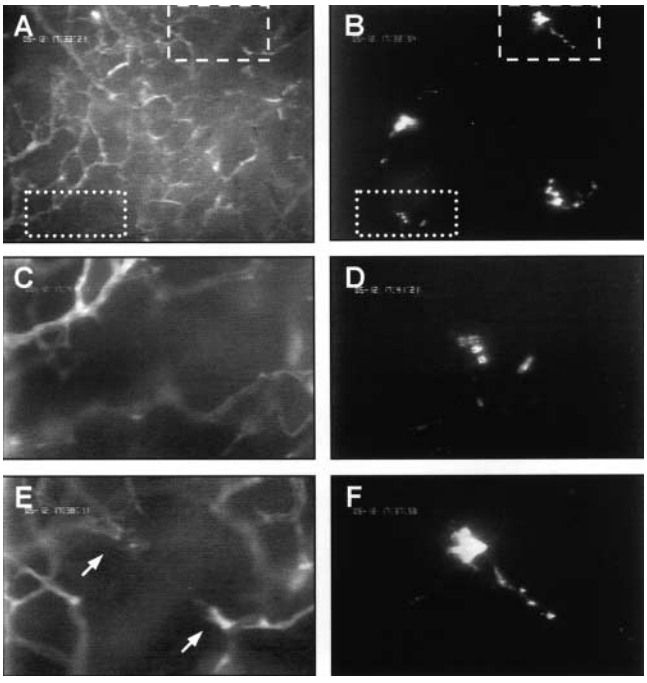

Figure 4. Morphological changes of eEPCs after extravasation on day one after injection. (A and B) Multicellular clusters of DiI-labeled eEPCs are located extravascularly throughout the tumor. Same regions of interest in A and B. Squares indicate areas highlighted in (C) and (D, dotted line) and (E) and (F, dashed line). (C–F) Higher magnification of tumor blood vessels (C and E) and extravascular eEPCs (D and F). eEPCs either showed a round (D) or elongated shape and displayed bipolar morphology (F). Note the intimate relationship of cell to angiogenic vascular sprouts (arrows). Tumor microvasculature visualized after contrast enhancement by FITC-dextran.

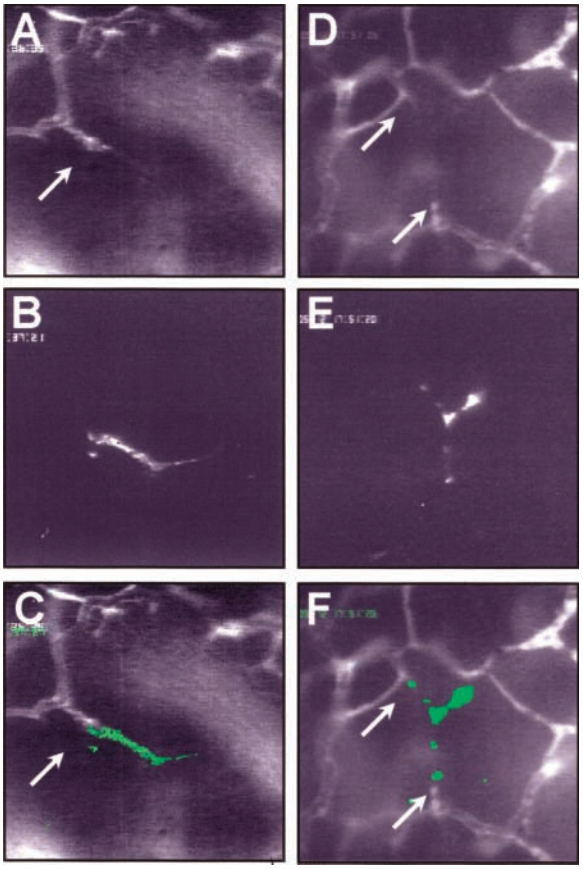

Figure 5. Extravasated eEPCs branch and interconnect tumor blood vessels. (A and D) Tumor microvasculature after contrast enhancement by FITC-dextran. (B and E) Same regions of interest as in A and D, demonstrating DiI-labeled eEPCs. (C and F) Superimposed FITC and DiI images after adding false colors to DiI images. eEPCs are marked with green false color. (A–C) eEPCs participate in angiogenic sprouting (arrow indicates vascular sprout; day 1 after injection). (D–F) eEPCs branch and span between individual tumor blood vessels interconnecting distant microvascular segments (arrows indicate vascular sprouts; day 1 after injection).

microvasculature immediately after systemic injection (Fig. 6 F). This became even more pronounced after 60 min, due to the continuing arrest of recirculating eEPCs. However, not only the recruitment of eEPCs was tumor-specific but also their extravasation, survival, and incorporation into functional tumor blood vessels by days 1 and 4. We noted with interest that not every arrested cell was finally incorporated. Rather, this process was characterized by ~30% angiogenic efficiency because ~55% of initially arrested cells extravasated and survived (day 1), and 30% finally formed functional tumor blood vessels (Fig. 6 F, day 4).

The tumor-specific incorporation of circulating eEPCs raised the question about the proportion of the neovasculature derived from the eEPCs versus that sprouting from preexisting vessels. To quantitate this, we counted the total number of eEPC-positive vascular sprouts (i.e., associated with incorporated eEPCs) and eEPC-negative vascular sprouts, and demonstrated that eEPCs contributed to 12% of newly forming tumor vessels. As a result, by day 4, incorporated eEPCs composed 3% of the total tumor vessel density.

To further address the specificity of angiogenic eEPC homing, we assessed their distribution within various organs by intravital fluorescence microscopy. After injection, we detected individual eEPCs within the liver (37 ± 2 mm^{-2}), spleen (20 ± 4 mm^{-2}), and lung (21 ± 2 mm^{-2}) representing organs that are characterized by a high organ blood flow and fenestrated endothelium. No eEPCs were found in the heart, pancreas, or kidney. In contrast to the angiogenic tumor microvasculature, all arrested eEPCs within organs retained their round morphology and were not incorporated into the endothelial lining of blood vessels.

Incorporation of eEPCs Does Not Enhance Tumor Vascularization and Growth. Incorporation of eEPCs into the tumor microvasculature may affect tumor angiogenesis, and thereby accelerate tumor vascularization and tumor growth. To test this possibility, we analyzed the total vessel density and area of the tumors before and 4 d after eEPC injection and compared them to tumors grown within the skinfold chamber but lacking circulating eEPCs. As demonstrated in Fig. 7 (A and B), incorporation of eEPCs however did not have a significant effect on the total vessel density and tumor size. The latter was further confirmed in subcutaneous xenografts revealing no difference in tumor volume between animals injected with PBS or eEPCs (Fig. 7 C).

Selectins and PSGL-1 Mediate Homing of Embryonic EPCs. Our results indicate that homing of circulating eEPCs to the tumor vasculature is determined by adhesive mechanisms reminiscent of the interaction of leukocytes with microvascular endothelium. To gain more insight into the underlying mechanisms, first we studied the expression of adhesion molecules in the tumor endothelium. Immunohistochemistry of the C6 tumors revealed strong expression of PECAM-1 (Fig. 8 A), moderate expression of P-selectin (Fig. 8 B), weak expression of E-selectin (Fig. 8 C; tumor periphery only), ICAM-1 and ICAM-2 (not depicted), and no expression of VCAM-1, PNAd, or MAdCAM-1. Second, we analyzed the expression of the cognate ligands by the eEPCs. RT-PCR analysis failed to show expression of the ligands for ICAM-1 and ICAM-2 (unpublished data), but demonstrated a strong expression of the E- and P-selectin ligands, ESL-1 and PSGL-1, respectively (Fig. 1 C). For PSGL-1, the expression of the protein on the cell surface could be confirmed by flow cytometry, albeit at low levels (Fig. 8 I), as compared with the mouse neutrophilic progenitor cell line 32DCl3 that was used as a positive control (not depicted; reference 29). This indicated that eEPCs have the ability to bind to E- and P-selectin. We tested this notion using E- and P-selectin IgG chimera proteins. As shown in Fig. 8 (E–H), both molecules bind to the eEPCs in a strong and specific manner demonstrating the presence of functional binding sites for both selectins on the cell surface.

Based on these results, next we addressed the significance of E- and P-selectin and PSGL-1 in mediating EPC homing to tumor vessels by using blocking antibodies directed against PSGL-1 or E- and P-selectin. Pretreatment of mice with an antibody cocktail directed simultaneously against

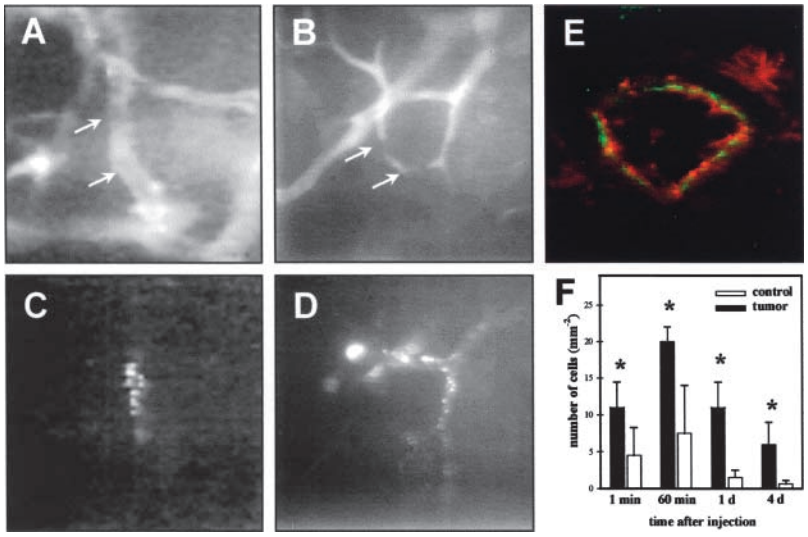

Figure 6. Functional incorporation of eEPCs into the tumor microvasculature on day 4 after injection. (A and B) Tumor microvasculature after contrast enhancement by FITC-dextran. (C and D) Same regions of interest as in A and B, demonstrating DiI-labeled eEPCs that line perfused tumor blood vessels, indicating successful incorporation into the new tumor microvasculature (arrows). (E) Cryosections of tumor specimens stained with fluorescent antibodies against PECAM-1 (red), confirming the successful integration of EGFP-labeled eEPCs (green) into the endothelial lining of the tumor microvasculature. (F) Quantitative analysis of eEPCs within tumor ($n = 9$ animals) and control tissue (control is chamber preparation of normal tissue without tumor cell implantation; $n = 4$ animals). Error bars show mean ± SD values. *, $P < 0.05$ versus control tissue.

E- and P-selectin, as well as pretreatment of eEPCs with an antibody directed against PSGL-1 before injection, reduced initial eEPC arrest on the tumor endothelium and subsequent eEPC incorporation into the tumor microvasculature by 76 and 78%, respectively (Fig. 8 J). However, those cells, which were arrested despite blocking PSGL-1 or E-/P-selectin, followed the subsequent multistep process of EPC incorporation, suggesting that selectin binding exclusively mediates the initial EPC arrest.

Discussion

We have shown that eEPCs, isolated at the onset of vasculogenesis, can function as endothelial progenitor cells in the adult environment and can contribute to tumor angiogenesis after systemic injection. The recruitment of eEPCs to tumor angiogenesis represents a multistep process, including (a) active arrest and homing of the circulating cells within the angiogenic microvasculature; (b) transendothelial extravasation into the interstitial space; (c) extravascular formation of cellular clusters; (d) creation of vascular sprouts and cellular networks; and (e) incorporation into a functional microvasculature. Finally, we have provided evidence that PSGL-1 and E- and P-selectin mediate homing of EPCs to the tumor endothelium. Thus, this paper provides the first insight into the mechanisms underlying EPC recruitment to angiogenic sites.

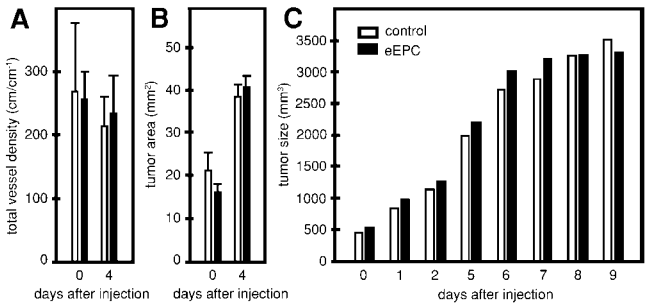

Figure 7. Effects of eEPC incorporation on tumor vascularization and tumor growth. Quantitative analysis of total vessel density (A) and tumor area (B) of C6 xenografts implanted into the skinfold chambers of nude mice. Measurements were performed in three to six regions of interest per tumor and per time point, before and 4 d after injection of eEPCs (eEPC, black bars; $n = 6$) or PBS (control, white bars; $n = 5$). Error bars show mean ± SD values. (C) Tumor growth curves for subcutaneous C6 xenografts implanted into the left flank regions of nude mice before and up to 9 d after injection of eEPCs (EPC, black bars; $n = 4$) or PBS (control, white bars; $n = 4$). Mean values are shown.

Our results raise fundamental issues about the biology of endothelial progenitor cells, taking into account the entirely different milieu of eEPC origin as compared with the transplantation site in this work. The cells originate from E7.5 embryos and express early endothelial genes, which match the expression profile of angioblasts located symmetrically at the area of the proximal lateral mesoderm, giving rise to the primitive endocardium and major blood vessels (13, 30). The fact that these cells can contribute to tumor angiogenesis indicates that eEPCs, although they are primarily programmed to form blood vessels during embryonic vascular development, retain this ability within an angiogenic environment in the adult.

Interestingly, cells identified recently within the side population of bone marrow–derived adult progenitor cells share striking gene expression profile similarities to the eEPCs (16). Accordingly, this adult $CD34^-$ cell subpopulation displays low flk-1 and low VE-cadherin expression, but high tie-2 and c-kit expression, suggesting that these cells might represent an equivalent to eEPC population in the adult. This last possibility will further enhance the use of eEPCs as an experimental tool to study the mechanisms underlying EPC recruitment during neovascularization. One advantage of this approach is that murine eEPCs supply an unlimited cell source that is easily amenable to ex vivo expansion and genetic manipulation. Furthermore, eEPCs represent an ideal system for a functional analysis of molecules involved in endothelial development and function because most of them are expressed or can be induced in the isolated cells.

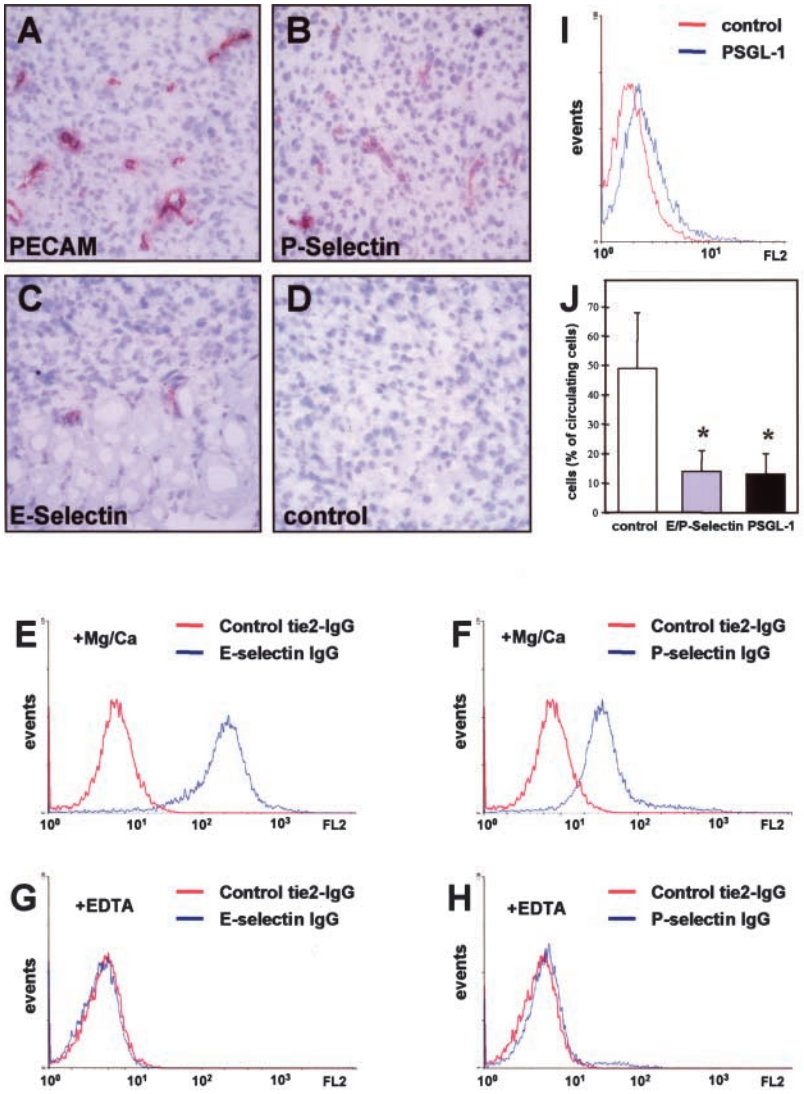

Figure 8. Interaction of eEPCs with tumor endothelium is mediated by selectins and PSGL-1. (A–D) Immunohistochemistry for PECAM-1 (A), P-selectin (B), E-selectin (C), and negative control (D) confirms P-selectin and E-selectin (the latter only in tumor periphery) expression by tumor endothelium. Tissue sections were counterstained with hematoxylin. (E–H) E- and P-selectins bind to eEPCs. Flow cytometry using an E-selectin IgG chimera (E) or a P-selectin IgG chimera (F) shows strong binding to eEPCs in the presence of Mg^{2+} and Ca^{2+} as compared with a tie2-IgG chimera control. The binding of both proteins is abolished in the presence of EDTA (G and H). (I) Flow cytometry demonstrates surface expression of the P-selectin ligand PSGL-1 in eEPCs. (J) Quantitative analysis of eEPC homing to tumor endothelium using intravital fluorescence videomicroscopy 10 min after cell injection and after blocking of PSGL-1, or P-selectin and E-selectin. $n = 3$ animals per experimental group. *, $P < 0.05$.

We have shown that the preferential homing of circulating eEPCs to the angiogenic tumor vasculature is determined by adhesive (i.e., active) mechanisms reminiscent of the interaction of activated leukocytes with microvascular endothelium (20, 31, 32). These similarities extend to the molecular level because expression analysis in the tumor endothelium and eEPCs, binding assays of chimeric molecules in vitro, and blocking experiments using specific antibodies in vivo, all demonstrate that selectins and their ligand PSGL-1 mediate the initial adhesion of the eEPCs to the tumor endothelium. We have also performed FACS® analysis on eEPCs using a large panel of antibodies that recognize other known cell adhesion molecules shown previously to direct interaction of leukocytes with the vascular wall (31, 32). The results showed that eEPCs do not express significant levels of VCAM-1, LFA-1, Mac-1, $\alpha_4\beta_1$ integrin, ICAM-1, ICAM-2, and PECAM-1. Therefore, the presence and identity of additional adhesion molecules on eEPCs that might be involved in their interaction with activated tumor endothelium remain currently unknown.

Adhesion of eEPCs to the tumor vessel endothelium may be further facilitated by the tumor-specific microhemodynamics, which are characterized by a much lower blood cell velocity (~350 μm/s) and wall shear stress (~4.0 dyne/cm^2) when compared with physiological conditions in postcapillary venules (23; our paper). This could explain an efficient eEPC arrest despite the relatively low levels of PSGL-1 detected by FACS® analysis. The observation that after permanent adhesion, eEPCs extravasate into the interstitium further indicates similar mechanisms underlying eEPC and leukocyte recruitment and migration through the endothelial lining. This is in contrast to a nonangiogenic microvasculature, where eEPCs are arrested by passive plugging of small caliber capillaries and remain intravascular.

After extravasation, we revealed two patterns of eEPC behavior. On the one hand, the cells formed small clusters, giving rise to cellular networks that were incorporated into the tumor microvasculature. Such network formation may facilitate tumor vascularization by bridging distinct vascular

beds. On the other hand, individual eEPCs were found to localize at sprouting sites. This may reflect either a particular adhesiveness in these areas and/or a special role of EPCs in sprout formation and guidance. These observations suggest a potential role for EPCs in orchestrating the process of angiogenesis, which would be in line with the recent finding that hematopoietic stem cells promote vessel sprouting in vitro and in vivo (33).

It is important to note that the experiments described in this paper were also performed with cells after they were differentiated to more mature endothelial cells in vitro (Fig. 1 C; reference 13), serving as a control for the progenitor cells. Interestingly, both the homing as well as the incorporation of the differentiated cells to the tumor microvasculature were lower when compared with undifferentiated cells, indicating that the progenitor phenotype is of importance in the multistep EPC recruitment. However, due to methodological problems, these experiments were not conclusive in that (a) markedly less differentiated than undifferentiated cells gained access to the control and tumor microvasculature; and (b) the systemic injection of differentiated cells often resulted in a macro- and microhemodynamic impairment and, finally, breakdown within a few minutes. The reason for this is not clear, but most likely it can be attributed to the fact that differentiated cells appear to be more "sticky" before injection, and, thus, being sequestered within the microvasculature of large organs (lung, liver, and spleen) and they impair microcirculation during their first passage.

In light of the results outlined here, one can now postulate a plausible model for EPC recruitment and function during tumor angiogenesis. As a first step, certain parameters in the blood (e.g., high VEGF levels) mobilize and enhance differentiation of hematopoietic stem cells toward the endothelial progenitor cell lineage (3, 8). At the same time, as yet unknown mechanisms activate endothelial cells in the vicinity of the angiogenic site so that they can bind circulating EPCs and guide them through the vascular wall into the interstitial tissue. There, EPCs form clusters, contribute to angiogenic sprout formation, and form networks that bridge preexisting blood vessels. Consequently, the model outlined here suggests that this multistep process of neovascularization via EPC recruitment is distinct from the classic processes of vasculogenesis (in situ assembly of blood vessels by endothelial cells differentiating from mesoderm), angiogenesis (proliferation, sprouting, and migration of endothelial cells from preexisting blood vessels), or vascular remodeling (intussusceptive vessel growth and rearrangement of vascular beds; reference 34). Therefore, we would like to propose the term "angiomorphosis" as the process of enhancing tissue vascularization through (a) active recruitment of EPCs from the circulation by endothelial cells and (b) the action of EPCs as organizers of the angiogenic process (from the Greek words "angio" for blood vessel and "morphosis" to give shape, to form). It will be interesting to test in future work if bone marrow–derived EPCs follow similar mechanisms. It is interesting to note that a recent paper showed that functional selectin ligands and selectins mediate interaction of hematopoietic $CD34^+$ stem cells with bone marrow endothelium (35). The $CD34^+$ stem cells are PSGL-1–positive, indicating that similar homing mechanisms are used by bone marrow stem cells.

Our results indicate a low level of eEPC engraftment for tumor angiogenesis, ~5% of all cells passing through the tumor microvasculature, but also shed some light on the reason for this angiogenic inefficiency. Although >40% of all the injected cells passing through the tumor microvasculature adhered permanently to the endothelium of the tumor blood vessels, most of the cells failed to extravasate and, thus, to incorporate into new blood vessels.

Analysis of tumor growth showed that incorporation of eEPCs did not have a significant effect on total vessel density and tumor size. The latter was further confirmed in additional experiments using subcutaneous C6 glioma xenografts that also revealed no difference in tumor growth between animals injected with PBS or eEPCs. However, it should be noted that the lack of an eEPC effect on tumor growth and vascularization may be only true for a single injection of cells, as performed in this work. It is also possible that the eEPC effect is tempered because the injected cells are competing with endogenous EPCs. In contrast, application of eEPCs into models of tissue ischemia has resulted in increased collateral vessel density, blood flow levels, and tissue function (unpublished data). This led us to conclude that eEPCs are recruited to angiogenic sites, but have a pronounced effect on vascular density only in highly ischemic areas where local angiogenesis is severely impaired. Thus, eEPCs may be used as a novel vehicle to treat tumors without stimulating tumor growth.

As aforementioned in the previous paragraph, a single injection of the eEPCs in this work did not exert significant effects on tumor growth and tumor vascularization. Therefore, we do not expect that blocking eEPC recruitment via selectin inhibition in this experimental design will significantly alter the course of tumor growth and vascularization. However, it has been observed that growth rates of primary tumors are significantly lower in P-selectin–deficient mice and that this was not related to a blocking of leukocyte infiltration (36). It is interesting to speculate that a diminished recruitment of autologous EPCs might be responsible for this observed phenomenon.

In summary, this paper provides first insights into the mechanisms underlying recruitment, homing, and vascular incorporation of circulating EPCs during tumor vascularization. The results are also of therapeutic interest because they set the basis for the design of novel means to manage blood vessel growth. A better understanding of eEPC biology will help to exploit these cells for somatic cell–based therapeutic approaches.

We would like to thank Dr. M.D. Menger for his help, Dr. G. Reisbach for advice on FACS® analysis, and A. Geishauser, M. Herbst, S. Mohr, and S. Merfeld-Clauss for excellent technical assistance.

This work was supported by the Deutsche Forschungsgemeinschaft Priority grant 1069 "Angiogenesis" (HA 2983/1-2 and VA 151/4-2), and the German Human Genome Project (DHGP 9907).

Submitted: 19 September 2002
Revised: 14 April 2003
Accepted: 6 May 2003

References

1. Asahara, T., H. Masuda, T. Takahashi, C. Kalka, C. Pastore, M. Silver, M. Kearne, M. Magner, and J.M. Isner. 1999. Bone marrow origin of endothelial progenitor cells responsible for postnatal vasculogenesis in physiological and pathological neovascularization. *Circ. Res.* 85:221–228.
2. Asahara, T., T. Takahashi, H. Masuda, C. Kalka, D. Chen, H. Iwaguro, Y. Inai, M. Silver, and J.M. Isner. 1999. VEGF contributes to postnatal neovascularization by mobilizing bone marrow-derived endothelial progenitor cells. *EMBO J.* 18:3964–3972.
3. Takahashi, T., C. Kalka, H. Masuda, D. Chen, M. Silver, M. Kearney, M. Magner, J.M. Isner, and T. Asahara. 1999. Ischemia- and cytokine-induced mobilization of bone marrow-derived endothelial progenitor cells for neovascularization. *Nat. Med.* 5:434–438.
4. Kalka, C., H. Masuda, T. Takahashi, R. Gordon, O. Tepper, E. Gravereaux, A. Pieczek, H. Iwaguro, S.I. Hayashi, J.M. Isner, and T. Asahara. 2000. Vascular endothelial growth factor(165) gene transfer augments circulating endothelial progenitor cells in human subjects. *Circ. Res.* 86:1198–1202.
5. Kalka, C., H. Masuda, T. Takahashi, W.M. Kalka-Moll, M. Silver, M. Kearney, T. Li, J.M. Isner, and T. Asahara. 2000. Transplantation of ex vivo expanded endothelial progenitor cells for therapeutic neovascularization. *Proc. Natl. Acad. Sci. USA.* 97:3422–3427.
6. Ikpeazu, C., M.K. Davidson, D. Halteman, P.J. Browning, and S.J. Brandt. 2000. Donor origin of circulating endothelial progenitors after allogeneic bone marrow transplantation. *Biol. Blood Marrow Transplant.* 6:301–308.
7. Peichev, M., A.J. Naiyer, D. Pereira, Z. Zhu, W.J. Lane, M. Williams, M.C. Oz, D.J. Hicklin, L. Witte, M.A. Moore, and S. Rafii. 2000. Expression of VEGFR-2 and AC133 by circulating human CD34(+) cells identifies a population of functional endothelial precursors. *Blood.* 95:952–958.
8. Gill, M., S. Dias, K. Hattori, M.L. Rivera, D. Hicklin, L. Witte, L. Girardi, R. Yurt, H. Himel, and S. Rafii. 2001. Vascular trauma induces rapid but transient mobilization of VEGFR2(+)AC133(+) endothelial precursor cells. *Circ. Res.* 88:167–174.
9. Lyden, D., K. Hattori, S. Dias, C. Costa, P. Blaikie, L. Butros, A. Chadburn, B. Heissig, W. Marks, L. Witte, et al. 2001. Impaired recruitment of bone-marrow-derived endothelial and hematopoietic precursor cells blocks tumor angiogenesis and growth. *Nat. Med.* 7:1194–1201.
10. Reyes, M., A. Dudek, B. Jahagirdar, L. Koodie, P.H. Marker, and C.M. Verfaillie. 2002. Origin of endothelial progenitors in human postnatal bone marrow. *J. Clin. Invest.* 109:337–346.
11. Blau, H.M., T.R. Brazelton, and J.M. Weimann. 2001. The evolving concept of a stem cell: entity or function? *Cell.* 105: 829–841.
12. Risau, W. 1997. Mechanisms of angiogenesis. *Nature.* 386: 671–674.
13. Hatzopoulos, A.K., J. Folkman, E. Vasile, G.K. Eiselen, and R.D. Rosenberg. 1998. Isolation and characterization of endothelial progenitor cells from mouse embryos. *Development.* 125:1457–1468.
14. Read, T.A., M. Farhadi, R. Bjerkvig, B.R. Olsen, A.M. Rokstad, P.C. Huszthy, and P. Vajkoczy. 2001. Intravital microscopy reveals novel antivascular and antitumor effects of endostatin delivered locally by alginate-encapsulated cells. *Cancer Res.* 61:6830–6837.
15. Asahara, T., T. Murohara, A. Sullivan, M. Silver, R. van der Zee, T. Li, B. Witzenbichler, G. Schatteman, and J.M. Isner. 1997. Isolation of putative progenitor endothelial cells for angiogenesis. *Science.* 275:964–967.
16. Jackson, K.A., S.M. Majka, H. Wang, J. Pocius, C.J. Hartley, M.W. Majesky, M.L. Entman, L.H. Michael, K.K. Hirschi, and M.A. Goodell. 2001. Regeneration of ischemic cardiac muscle and vascular endothelium by adult stem cells. *J. Clin. Invest.* 107:1395–1402.
17. Jain, R.K., K. Schlenger, M. Hockel, and F. Yuan. 1997. Quantitative angiogenesis assays: progress and problems. *Nat. Med.* 3:1203–1208.
18. Vajkoczy, P., A. Ullrich, and M.D. Menger. 2000. Intravital fluorescence videomicroscopy to study tumor angiogenesis and microcirculation. *Neoplasia.* 2:53–61.
19. Vajkoczy, P., L. Schilling, A. Ullrich, P. Schmiedek, and M.D. Menger. 1998. Characterization of angiogenesis and microcirculation of high-grade glioma: an intravital multifluorescence microscopic approach in the athymic nude mouse. *J. Cereb. Blood Flow Metab.* 18:510–520.
20. Vajkoczy, P., M. Laschinger, and B. Engelhardt. 2001. Alpha4-integrin-VCAM-1 binding mediates G protein-independent capture of encephalitogenic T cell blasts to CNS white matter microvessels. *J. Clin. Invest.* 108:557–565.
21. Von Andrian, U.H., P. Hansell, J.D. Chambers, E.M. Berger, I. Torres Filho, E.C. Butcher, and K.E. Arfors. 1992. L-selectin function is required for beta 2-integrin-mediated neutrophil adhesion at physiological shear rates in vivo. *Am. J. Physiol.* 263:H1034–H1044.
22. Ley, K., and P. Gaehtgens. 1991. Endothelial, not hemodynamic, differences are responsible for preferential leukocyte rolling in rat mesenteric venules. *Circ. Res.* 69:1034–1041.
23. Vajkoczy, P., M. Farhadi, A. Gaumann, R. Heidenreich, R. Erber, A. Wunder, J.C. Tonn, M.D. Menger, and G. Breier. 2002. Microtumor growth initiates angiogenic sprouting with simultaneous expression of VEGF, VEGF receptor-2, and angiopoietin-2. *J. Clin. Invest.* 109:777–785.
24. Laschinger, M., and B. Engelhardt. 2000. Interaction of alpha4-integrin with VCAM-1 is involved in adhesion of encephalitogenic T cell blasts to brain endothelium but not in their transendothelial migration in vitro. *J. Neuroimmunol.* 102:32–43.
25. Vecchi, A., C. Garlanda, M.G. Lampugnani, M. Resnati, C. Matteucci, A. Stoppacciaro, H. Schnurch, W. Risau, L. Ruco, A. Mantovani, et al. 1994. Monoclonal antibodies specific for endothelial cells of mouse blood vessels. Their application in the identification of adult and embryonic endothelium. *Eur. J. Cell Biol.* 63:247–254.
26. Hallmann, R., D.N. Mayer, E.L. Berg, R. Broermann, and E.C. Butcher. 1995. Novel mouse endothelial cell surface marker is suppressed during differentiation of the blood brain barrier. *Dev. Dyn.* 202:325–332.
27. Austrup, F., D. Vestweber, E. Borges, M. Löhning, R. Bräuer, U. Herz, H. Renz, R. Hallman, A. Scheffold, A. Radbruch, and A. Hamann. 1997. P- and E-selectin mediate recruitment of T-helper-1 but not T-helper-2 cells into inflamed tissues. *Nature.* 385:81–83.
28. Borges, E., W. Tietz, M. Steegmaier, T. Moll, R. Hallmann,

A. Hamann, and D. Vestweber. 1997. P-selectin glycoprotein ligand-1 (PSGL-1) on T helper 1 but not on T helper 2 cells binds to P-selectin and supports migration into inflamed skin. *J. Exp. Med.* 185:573–578.
29. Valtieri, M., D. Santoli, D. Caracciolo, B.L. Kreider, S.W. Altmann, D.J. Tweardy, I. Gemperlein, F. Mavilio, B. Lange, and G. Rovera. 1987. Establishment and characterization of an undifferentiated human T leukemia cell line which requires granulocyte-macrophage colony stimulatory factor for growth. *J. Immunol.* 138:4042–4050.
30. Hatzopoulos, A.K., and R.D. Rosenberg. 1999. Embryonic development of the vascular system. *In* Angiogenesis and Cardiovascular Disease. J.A. Hare and M. Simons, editors. Oxford University Press, New York, Oxford. 3–29.
31. Butcher, E.C. 1991. Leukocyte-endothelial cell recognition: three (or more) steps to specificity and diversity. *Cell.* 67: 1033–1036.
32. Menger, M.D., and B. Vollmar. 1996. Adhesion molecules as determinants of disease: from molecular biology to surgical research. *Br. J. Surg.* 83:588–601.
33. Takakura, N., T. Watanabe, S. Suenobu, Y. Yamada, T. Noda, Y. Ito, M. Satake, and T. Suda. 2000. A role for hematopoietic stem cells in promoting angiogenesis. *Cell.* 102: 199–209.
34. Carmeliet, P. 2000. Mechanisms of angiogenesis and arteriogenesis. *Nat. Med.* 6:389–395.
35. Hidalgo, A., L.A. Weiss, and P.S. Frenette. 2002. Functional selectin ligands mediating human CD34+ cell interactions with bone marrow endothelium are enhanced postnatally. *J. Clin. Invest.* 110:559–569.
36. Kim, Y.J., L. Borsig, N.M. Varki, and A. Varki. 1998. P-selectin deficiency attenuates tumor growth and metastasis. *Proc. Natl. Acad. Sci. USA.* 95:9325–9330.